small deviations from thermodynamic equilibrium then the local equilibrium assumption of AT is unnecessary.

We now compare our result for the BCS limit Eqs. (7) and (8) with the result of AT.[27] It is stated there that AT Eq. (4.6) is valid when $\Omega > 2\Delta$ but this is incorrect. An additional requirement is $v_F q > \Omega$, where v_F is the Fermi velocity and $1/q$ is the characteristic length of the spatial variation of the order parameter. Our result for the BCS limit is for the case $\Omega > 2\Delta$, $q=0$. The expression of AT must be modified in this case to include a term of order Δ^2 which they have dropped in their kernel $L(0, 0)$. If this correction is made, the results agree. The value for the relaxation rate of AT as quoted by Lucas and Stephen[28] is therefore incorrect and should be replaced by the expression $1/\tau_a = 4\Delta$.

We conclude by commenting on the result of AT in the diffusion regime $v_F q > \Delta > \Omega$. If we linearize their Eq. (4.6) about equilibrium near T_c we find

$$-\lambda \delta\Delta = (\partial/\partial t - D\nabla^2)\Delta, \qquad (12)$$

where

$$\lambda = 14\zeta(3)\Delta^2/\pi^3 k T_c, \qquad D = 7\zeta(3) v_F^2/6\pi^3 k T_c.$$

Since $\lambda/Dq^2 = 12(\Delta/v_F q)^2$, we may neglect the left-hand side of Eq. (12). We then have a simple diffusion equation with a constant diffusion coefficient and a diffusion rate $\Omega = Dq^2$. The range of validity is then $kT_c > v_F q > \Delta > Dq^2$. There is no anomalous behavior of D as $T \to T_c$ but it should be pointed out that the maximum value of q for which the diffusion equation is valid decreases to zero as the critical point is approached.

[27] Reference 4, Eq. (4.6).
[28] Reference 8, Eq. (38).

PHYSICAL REVIEW VOLUME 169, NUMBER 2 10 MAY 1968

Cylindrically Symmetric Solutions of the Ginzburg-Landau Equations*

PAUL THOLFSEN† AND HANS MEISSNER
Department of Physics, Stevens Institute of Technology, Hoboken, New Jersey

(Received 6 November 1967)

The Ginzburg-Landau questions have been solved for an isolated magnetic flux line enclosing a single flux quantum. The radial dependence of the magnetic field H, the order parameter n_s, the current density J, and the resulting free energy per unit length F/L, are obtained for values of the Ginzberg-Landau parameter $\kappa = 20$, 5, 1.0, 0.5, and 0.2. For $\kappa \lesssim 5$, the axial magnetic field $H(0)$ is approximately given by $H(0) = 0.62\kappa^{-0.43}\sqrt{2}H_{cb}$. The maximum value of the current density is approximately $J = 0.33\sqrt{2}H_{cb}/\lambda$, where H_{cb} is the bulk critical field and λ is the superconducting penetration depth.

I. INTRODUCTION

THE quantized flux tube is central to the present understanding of the behavior of type-II superconductors.[1–5] The structure of the flux tube was first treated by Abrikosov.[6] He set up the Ginsburg-Landau[7] (GL) equations for the cylindrically symmetric case, which corresponds to an isolated flux tube. Analytic solutions were then obtained for values of the GL parameter $\kappa \gg 1$. If this condition is not met, numerical analysis is required. Computer solutions have been obtained by Fink and Presson[8] and by Doll and Graf[9] for a fluxoid in a material for which $\kappa \lesssim 1$. However, these solutions were for a fluxoid inside a wire of finite diameter and therefore represent a different set of boundary conditions than that for an isolated flux tube.

We are presently investigating the behavior of thin, type-I, superconducting films in the presence of a perpendicular magnetic field. In this situation a flux tube structure is also exhibited.[10,11] We have investigated the behavior of the solutions of Abrikosov's equations for the isolated flux tube for several values of κ in the range from 0.2 to 20. We are primarily interested in the radial behavior of the order parameter and of the magnetic field for values of $\kappa < 1/\sqrt{2}$. However, we have also determined the current density distribution and the free energy per unit length of the isolated flux tube. Harden

* Supported by a grant from the National Science Foundation.
† National Science Foundation Trainee.
[1] P. W. Anderson and Y. B. Kim, Rev. Mod. Phys. **36**, 39 (1964).
[2] Y. B. Kim, C. F. Hempstead, and A. R. Strnad, Phys. Rev. **139**, 1163 (1965).
[3] J. Bardeen and M. J. Stephen, Phys. Rev. **140**, 1197 (1965).
[4] P. Nozieres and W. F. Vinen, Phil. Mag. **14**, 667 (1966).
[5] Albert Schmid, Physik Kondensierten Materie **5**, 301 (1966).
[6] A. A. Abrikosov, Zh. Eksperim. i Teor. Fiz. **32**, 1442 (1957) [English transl.: Soviet Phys.—JETP **5**, 1174 (1957)].
[7] V. L. Ginsburg and L. D. Landau, Zh. Eksperim i Teor. Fiz. **20**, 1064 (1950).
[8] H. J. Fink and A. G. Presson, Phys. Rev. **151**, 219 (1966).
[9] R. Doll and P. Graf, Z. Physik **197**, 172 (1966).
[10] M. Tinkham, Phys. Rev. **129**, 2413 (1963).
[11] D. St. James and P. G. de Gennes, Phys. Letters **7**, 306 (1963).

TABLE I. Results of computer solutions.

κ	$h(0)$	$f(0)$	ϵ	j_{max}	r_{jm}	ρ	$\kappa\rho$	$h(1)/h(0)$	$h(2)/h(0)$
0.2	1.22	0.274	72	0.377	1.71	8.0	1.60	0.861	0.564
0.5	0.813	0.475	21	0.331	1.25	4.1	2.05	0.765	0.384
1.0	0.617	0.777	7.5	0.321	0.92	2.4	2.40	0.642	0.240
5.0	0.307	3.06	0.54	0.323	0.31	0.65	3.25	0.283	0.077
20	0.138	11.7	0.042	0.325	0.090	0.18	3.60	0.157	0.048

and Arp[12] have calculated H_{c1} of type-II superconductors, which is proportional to the free energy per unit length, and their data have been used for comparison purposes.

We are especially concerned with the details of the model of the flux tube which describes the central region as a core of radius, $R=\xi=\lambda/\kappa$, surrounded by a region of magnetic field with radius of order λ. We will show that the radial dependencies of the order parameter and the magnetic field for different values of κ do not scale in such a simple fashion.

II. METHOD OF SOLUTION

Abrikosov[6] starts with the GL equations written in the dimensionless reduced GL units in which length, vector potential, magnetic field, current density, flux, and free energy per unit length are normalized respectively as

$$r=R/\lambda, \tag{1a}$$

$$a=A/\sqrt{2}H_{cb}\lambda, \tag{1b}$$

$$h=H/\sqrt{2}H_{cb}, \tag{1c}$$

$$j=J/(\sqrt{2}H_{cb}/\lambda), \tag{1d}$$

$$\phi=\Phi/\sqrt{2}H_{cb}\lambda^2, \tag{1e}$$

$$\epsilon=(F/L)/(H_{cb}^2\lambda^2/4\pi), \tag{1f}$$

where H_{cb} is the bulk critical field. The GL parameter κ is defined by

$$\kappa=(2\sqrt{2}e/\hbar c)H_{cb}\lambda^2=2\pi(\sqrt{2}H_{cb}\lambda^2/\Phi_0), \tag{1g}$$

where Φ_0 is the flux quantum $hc/2e$, and h, e, and c have their usual meanings. In addition, Abrikosov introduces the quantities

$$f=\Psi(r)/\Psi(\infty) \tag{2}$$

and

$$Q=|\mathbf{a}-\nabla\varphi/\kappa|, \tag{3}$$

where φ is the phase of the wave function, $\Psi=fe^{i\varphi}$.

He shows that for a system enclosing a single quantum of flux, the GL equations may be written as

$$-(1/\kappa^2 r)(d/dr)(rdf/dr)+Q^2f=f-f^3 \tag{4}$$

and

$$d/dr[r^{-1}d/dr(rQ)]=Qf^2=-dh/dr=j. \tag{5}$$

For the variables f and Q, the set of boundary conditions defining the isolated flux tube is

$$f(r\to\infty)=1, \tag{6a}$$

$$Q(r\to\infty)=0, \tag{6b}$$

$$f(0)=0, \tag{6c}$$

$$Q(r\to 0)=1/\kappa r. \tag{6d}$$

It is convenient for us to define a new variable

$$p=Qr, \tag{7}$$

which, when substituted in Eqs. (4) and (5), results in

$$f''=\kappa^2(f^3-f)+(1/r)[(\kappa^2p^2f/r)-f'], \tag{8}$$

$$p''=(p'/r)+pf^2, \tag{9}$$

$$h=-p'/r, \tag{10}$$

and

$$j=pf^2/r, \tag{11}$$

where primes signify differentiation with respect to r. Similarly, the boundary conditions become[13]

$$f(r\to\infty)=1, \tag{12a}$$

$$p(r\to\infty)=0, \tag{12b}$$

$$f(0)=0, \tag{12c}$$

$$p(0)=1/\kappa. \tag{12d}$$

However, numerical integration requires the specification both of the values of the variables f and p and of their derivatives at $r=0$. Thus, $f'(0)$ and $p'(0)$ must be chosen to satisfy the boundary conditions at infinity. Rather than specifying $p'(0)$ we find it more convenient to specify $[p'/r]_{r=0}=-h(0)$.

A good check on the accuracy of the solutions is provided by the calculation of the flux in the flux tube. This is defined by

$$\phi=\int_0^\infty h(r)2\pi r dr. \tag{13}$$

Substitution of Eqs. (5), (6b), and (6d) into Eq. (13) gives

$$\phi=2\pi\int_0^\infty (d/dr)(rQ)dr=2\pi/\kappa \tag{14}$$

[12] J. L. Harden and V. Arp, Cryogenics 3, 105 (1963).

[13] This condition follows if one requires that the flux tube carry a single quantum of flux; see Eq. (13).

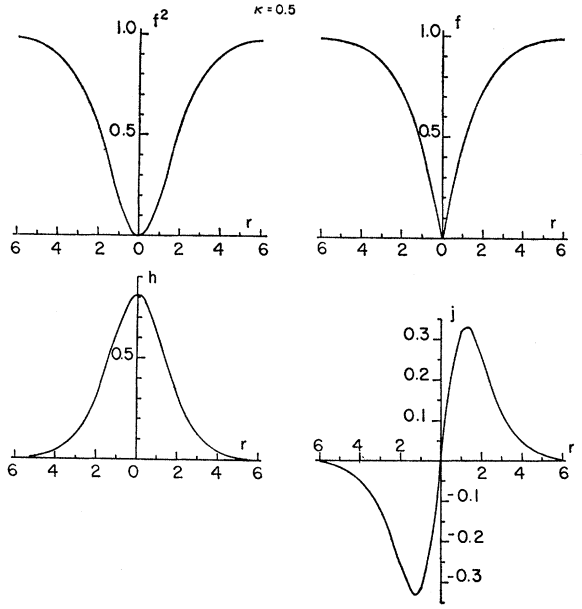

FIG. 1. Radial cross section of f^2, f, h, and j for $\kappa=0.5$.

[which is equivalent to a single quantum of flux in the reduced units of Eq. (1e)].

The free energy per unit length of flux line is given by Abrikosov[6] as

$$\epsilon=\int_0^\infty [h^2+\tfrac{1}{2}(1-f^4)]2\pi r dr. \qquad (15)$$

The integrals (13) and (15) are easily evaluated during the course of the numerical calculations required to determine $h(r)$ and $f(r)$.

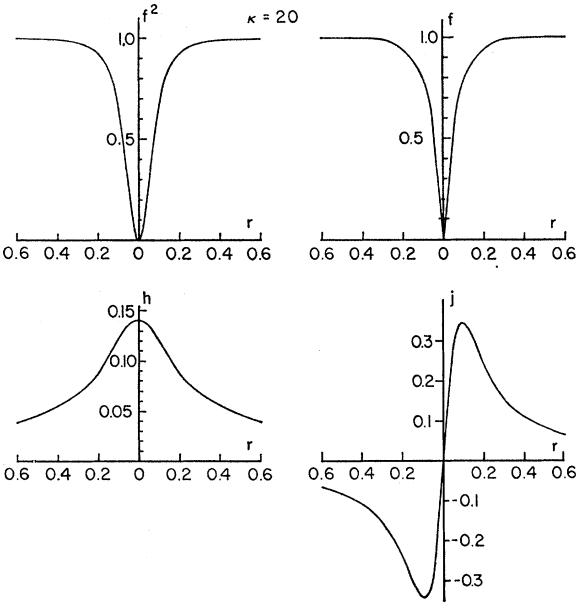

FIG. 2. Radial cross section of f^2, f, h, and j for $\kappa=20$.

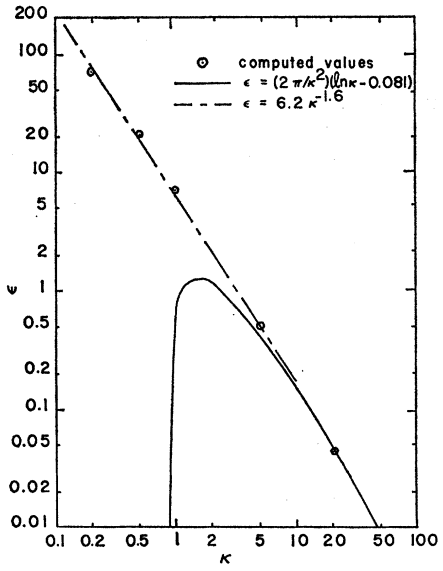

FIG. 3. Free energy per unit length ϵ, versus κ, with Abrikosov approximation [Eq. (16)] and small κ approximation [Eq. (18)].

Equations (8) and (9) are solved by means of an iterative numerical process. A fourth-order Runge-Kutta method[14] is carried out on an IBM 360/40 computer. The boundary conditions $f'(0)$ and $h(0)$ must be assumed in order to perform the solution. The initial approximation of these boundary conditions is made with the help of an examination of the boundary conditions corresponding to values of κ for which the solu-

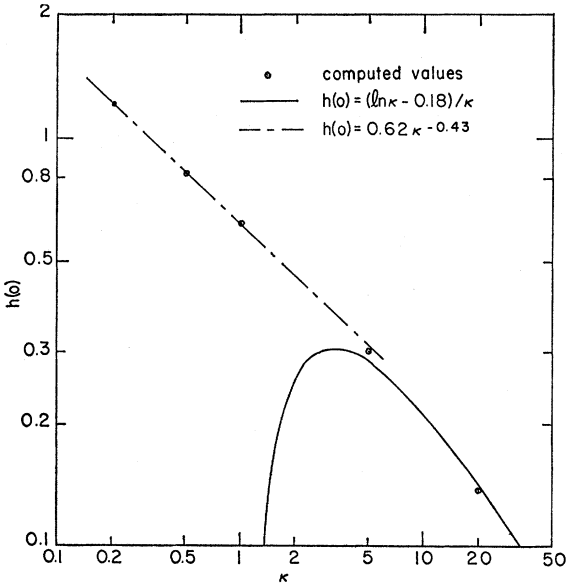

FIG. 4. Axial magnetic field $h(0)$, versus κ, with Abrikosov approximation [Eq. (17)] and small κ approximation [Eq. (19)].

[14] J. B. Scarborough, *Numerical Mathematical Analysis* (Johns Hopkins Press, Baltimore, 1964), 6th ed., p. 363.

tions have already been found. A suitable extrapolation or interpolation procedure is then used to estimate the approximate values of $f'(0)$ and $h(0)$.

The accuracy of the values of f and p at each point is tested in the following manner: Initially, r is increased by an amount δr_0 and both $p_0=p(r+\delta r_0)$ and $f_0=f(r+\delta r_0)$ are calculated. A set of closer approximations, $p_n(r+\delta r_0)$ and $f_n(r+\delta r_0)$, may be generated by first carrying out n successive halvings of δr_0 and then using the resulting value $\delta r_n=\delta r_0/2^n$ to perform 2^n successive Runge-Kutta calculations. The computer automatically repeats this process for $n=1$, 2, 3, etc., until both differences p_n-p_{n-1} and f_n-f_{n-1} are less than a specified amount. The accuracy check then ends and the computer uses f_n and p_n as starting values for the next interval. Equations (10) and (11) are used to calculate h and j at each point. The integrals (13) and (15) are evaluated by the trapezoidal method during the course of the calculation.

III. RESULTS

Solutions were obtained for values of $\kappa=0.2$, 0.5, 1.0, 5, and 20. The behavior of both $f(r)$ and $h(r)$ is quite unstable. A very small change in either of the boundary conditions $f'(0)$ or $h(0)$ (sometimes in the fifth decimal place) can cause $f(r)$ and/or $h(r)$ to diverge. An examination of Eq. (8) shows that the leading term on the right changes sign when f exceeds unity and, particularly in the case of large κ, causes f'' to increase rapidly. This results in a rapid growth of p'', as seen in Eq. (9).

Because of the sensitivity of the solutions to the values of $f'(0)$ and $h(0)$, it is costly to achieve a high accuracy. Their values shown in Table I are accurate to the three significant figures shown. The integrand in Eq. (15), however, has a significant value at rather large values of r. The term $\frac{1}{2}(1-f^4)$ is particularly sensitive to small departures of f from unity. Thus, in the case of the integration for ϵ, the second significant figure may be in error by one unit. For our purposes, this accuracy is sufficient. The resulting values of $h(0)$, $f'(0)$, ϵ, $j_{\max}$, and r_{jm}, the radius corresponding to $j_{\max}$, are tabulated in Table I. Plots of $f(r)$, $f^2(r)=n_e$ (the order parameter), $j(r)$, and $h(r)$ are shown in Figs. 1 and 2 for values of $\kappa=0.5$ and $\kappa=20$.

Abrikosov derived the following two expressions, for ϵ and the axial magnetic field $h(0)$, valid for $\kappa\gg1$:

$$\epsilon=(2\pi/\kappa^2)(\ln\kappa+0.081) \qquad (\kappa\gg1) \qquad (16)$$

and

$$h(0)=(\ln\kappa-0.18)/\kappa \qquad (\kappa\gg1). \qquad (17)$$

These expressions are plotted on logarithmic coordinates in Figs. 3 and 4, respectively, together with the results of our calculations for the range $20\geq\kappa\geq0.2$. It can be seen that the computer solutions and the expressions (16) and (17) are in good agreement for values of $\kappa\geq10$. For $10\geq\kappa\geq0.2$, a reasonable set of approximation formulas are

$$\epsilon\approx6.2\kappa^{-1.6} \qquad (10\geq\kappa\geq0.2) \qquad (18)$$

and

$$h(0)\approx0.62\kappa^{-0.43} \qquad (10\geq\kappa\geq0.2). \qquad (19)$$

These equations are also plotted in Figs. 3 and 4, respectively. The energy per unit length is proportional[6] to H_{c1}:

$$H_{c1}=\epsilon\kappa/4\pi, \qquad (20)$$

and our plot in Fig. 4 is thus equivalent to a plot of H_{c1} versus κ. A plot of the latter dependence has been presented by Harden and Arp[12] and our results are in good agreement with theirs, providing a good over-all check.

The solutions for $f(r)$ and $h(r)$ indicate a scaling of the flux tube, which differs from the core model described above. Defining the core radius as, for example, $\rho=r$ $(f=0.95)$, we expect that this radius should be proportional to $1/\kappa$. This is equivalent to $\kappa\rho=$ const. We find that this presumed proportionality does not exist, as is shown by the tabulation of values of $\kappa\rho$ in Table I.

In a similar manner, the notion of a magnetic field region with radius of order $R=\lambda$ (or $r=1$) implies that for all κ, ratios like $h(r=1)/h(0)$ should be reasonably constant. This would insure a structure with dimensions that scale as λ. We find, however, that the ratio has a very strong κ dependence, as shown in Table I. Closer examination shows that $h(1)/h(0)$ decreases with increasing κ, approximately as $1/\ln\kappa$. Ratios of the fields at two large radii, for example $h(20)/h(10)$, are more constant. However, this in itself is not significant because the behavior at such large radii is of little interest.

An interesting result of the numerical solutions for $j(r)$ is that $j_{\max}\approx0.33$ ($J=0.33\sqrt{2}H_{cb}/\lambda$ in conventional units) and is rather independent of κ. The corresponding values of r, however, are strongly κ-dependent. Both $j_{\max}$ and r_{jm} are tabulated in Table I.

In conclusion, we note that the use of the tabulated values of $f'(0)$ and $h(0)$ greatly simplifies the trial and error search required to find the boundary conditions for values of κ other than those used here. In the solutions presented here, the most time was spent in narrowing $f'(0)$ and $h(0)$ down to the first two significant figures. For greater accuracy, linear interpolation schemes become feasible.

ACKNOWLEDGMENTS

The authors wish to express their thanks to the staff of the Stevens Computer Center, and to Dr. Roger Pinkham for assistance with the calculations. The work was supported by a grant from the National Science Foundation. One of us (PT) wishes to acknowledge an NSF Traineeship.